IL NUOVO CIMENTO **45 C** (2022) 45
DOI 10.1393/ncc/i2022-22045-4

Colloquia: IWM-EC 2021

Comparison of heavy-ion transport simulations for mean-field dynamics

M. Colonna and the TMEP Collaboration

INFN, Laboratori Nazionali del Sud - Catania, Italy

received 12 May 2022

Summary. — Within the transport model evaluation project (TMEP) of simulations for heavy-ion collisions, the mean-field response is described here. Specifically, zero-sound propagation is considered for neutron-proton symmetric matter enclosed in a periodic box, at zero temperature and around normal density. The results of several transport codes belonging to two families (BUU-like and QMD-like codes) are compared among each other. QMD-like codes, using molecular dynamics methods, are characterized by large damping effects, attributable to the fluctuations inherent in their phase-space representation, and by slower density oscillations, as compared to BUU-like codes. The latter problem is mitigated in the more recent lattice formulation of some of the QMD codes.

1. – Introduction

Heavy-ion collisions offer unique possibilities to investigate, in laboratory conditions, nuclear matter away from saturation properties. The challenge is to connect the nuclear states of interest to the final experimental observables, so that information on the Equation of State (EoS) can be obtained. Transport approaches are the main tool to describe dissipative nuclear reactions and extract this information. Therefore, the reliability of transport models and the robustness of their predictions is important in heavy-ion research. It has recently become apparent that different conclusions could be drawn from the same data by relying on transport simulations, *e.g.*, in the investigations of isospin equilibration in peripheral collisions (isospin diffusion) or in the interpretation of ratios of charged pions. See [1] for a recent review. These discrepancies could naturally derive from the different approximation schemes, adopted in the different transport models, to deal with the quantum many-body problem or from differences in various technical assumptions. The impacts of the numerical details on predictions and conclusions are often difficult to discern. This situation led to the idea of a systematic comparison and evaluation of transport codes under controlled conditions, to eventually provide benchmark calculations and thus to improve the ability to reach robust conclusions from the comparison of transport simulations with experimental data.

Previous studies along this direction were dedicated to the comparison of transport model predictions for Au + Au collisions [2, 3]. A large part of the observed differences in the predicted reaction path and corresponding observables (such as collective flows) resulted from differences in the initialization of the systems and in the treatment of the collision integral (mainly Pauli blocking effects). The mean-field dynamics also seemed to play a role. However, the origins of the differences were often difficult to pin down unambiguously, since various effects interplay and propagate.

Significant progress in understanding the behavior of the different transport codes was made with subsequent studies, based on box calculations, *i.e.*, simulations of nuclear matter enclosed in a box with imposed periodic boundary conditions [4, 5]. In particular, the box calculations have the advantage that the different aspects of heavy-ion collisions can be isolated and tested separately, *e.g.*, the description of N-N scattering processes (*i.e.*, two-body correlations) and the mean-field dynamics. Here we report on the recent investigation of the mean-field dynamics [6], which involved fourteen transport models (see table I of ref. [6] for a full list and references).

2. – Transport approaches

The primary methodology for the dynamics of nuclear collisions at Fermi/intermediate energy are semi-classical transport theories, such as the Nordheim approach, in which the Vlasov equation for the one-body phase space distribution, $f(\vec{r}, \vec{p}; t)$, is extended with a Pauli-blocked Boltzmann collision term, which accounts for the average effect of the two-body residual interaction. The resulting transport equation is often called the Boltzmann-Uehling-Uhlenbeck (BUU) equation. In order to introduce fluctuations and further (many-body) correlations in the treatment of the reaction dynamics, a number of different avenues have been undertaken, which can be differentiated into two classes (see refs. [1, 7, 8] for recent reviews). One is the class of quantum molecular dynamics (QMD) models [9], while the other kind is represented by stochastic extensions of mean-field approaches of the BUU type [1, 10].

2·1. *BUU-like models.* – In BUU-like approaches, the time evolution of the distribution function, $f(\vec{r}, \vec{p}; t)$, follows the equation

$$\left(\frac{\partial}{\partial t} + \vec{\nabla}_p \epsilon \cdot \vec{\nabla}_r - \vec{\nabla}_r \epsilon \cdot \vec{\nabla}_p\right) f(\vec{r}, \vec{p}; t) = I_{coll}(\vec{r}, \vec{p}; t), \tag{1}$$

where $\epsilon[f]$ is the single-particle energy, usually derived from a density functional, and I_{coll} is the (stochastic) two-body collision integral, specified by an in-medium cross section $\mathrm{d}\sigma^{med}/\mathrm{d}\Omega$. In the present study, we focus on the mean-field propagation, thus we neglect the r.h.s. of eq. (1) and any fluctuation terms. It should be noticed that the BUU theory can more generally be formulated in a relativistic framework, and actually most codes in this comparison use a relativistic formulation. To this purpose, let us introduce a vector field $A^\mu(j^\mu)$, depending on the baryon current j^μ (whose fourth component coincides with the nucleon density ρ), and a scalar field $\Phi(\rho_S)$, that is a function of the scalar density ρ_S. Then the single-particle energy in eq. (1) can be expressed as: $\epsilon = E^* + A^0$, where $E^* = \sqrt{\vec{p^*}^2 + m^{*2}}$, with $p^{*\mu} = p^\mu - A^\mu$ and $m^* = M - \Phi$ (being M the nucleon mass).

It should be noted that, in the non-relativistic formulation of the nuclear interaction, the single-particle energy reduces to $\epsilon = \sqrt{\vec{p}^2 + M^2} + A^0(\rho)$ (for the local interactions considered here). The integro-differential non-linear BUU equation is solved numerically. To this end, the distribution function is represented in terms of finite elements, the so-called test particles (TP), characterized by time-dependent centroid coordinates and momenta $\vec{R}_i$ and $\vec{P}_i$. The number of TPs per nucleon is set to $N_{TP} = 100$ in this work. Upon this ansatz, the left-hand side of eq. (1) leads to Hamiltonian equations of motion for the TP centroid propagation:

$$\frac{\mathrm{d}\vec{R}_i}{\mathrm{d}t} = \vec{\nabla}_{P_i}\epsilon \quad \text{and} \quad \frac{\mathrm{d}\vec{P}_i}{\mathrm{d}t} = -\vec{\nabla}_{R_i}\epsilon. \tag{2}$$

2$\cdot$2. *QMD Models.* – In QMD models, the many-body state is represented by a simple product wave function of single-particle states with or without antisymmetrization [8,9]. The single-particle wave functions ϕ_i are usually assumed to have a fixed Gaussian shape,

$$\phi_i(\vec{r}_i;t) = \frac{1}{\left[2\pi(\Delta x)^2\right]^{\frac{3}{4}}} \exp\left[-\frac{[\vec{r}_i - \vec{R}_i(t)]^2}{4(\Delta x)^2}\right] e^{(i/\hbar)\vec{P}_i(t)\cdot\vec{r}_i}. \tag{3}$$

The time evolution of nuclear dynamics is formulated in terms of the changes in nucleon coordinates and momenta, similar to classical molecular dynamics, which are the centroids of the wave packets. This strategy yields equations of motion for the coordinates of the wave packets of similar form as obtained for the TPs in BUU. Though the nucleon wave functions are independent (mean-field approximation), the use of localised wave packets induces classical many-body correlations both in the mean-field propagation and two-body in-medium scattering (collision integral), where the latter is treated stochastically. This represents the main difference between BUU-like and QMD-like methods. In the philosophy of QMD one wants to go beyond the mean-field approach and include correlations and fluctuations from the beginning. However, these fluctuations, which are essentially of classical nature, can lead to a loss of the fermionic character of the system more rapidly than in BUU, as it was studied in ref. [4]. The fluctuations in QMD-type codes are regulated and smoothed by choosing parameter Δx, the width of the wave packet, cf. eq. (3). The effects of this difference in the amount of fluctuations between the two approaches will clearly be seen in the comparisons that follow.

3. – Results and discussions

A dedicated homework has been devised to test the mean-field propagation under controlled situations in the different transport codes.

We consider uniform symmetric matter at saturation density $\rho_0 = 0.16\,\mathrm{fm}^{-3}$ and zero temperature. For the cubic box employed (of size $L_\alpha = 20\,\mathrm{fm}$), this corresponds to $A = 1280$ nucleons. The system is initialized by impressing a sinusoidal distortion with wave number $k_{ini} = 2\pi/L_\alpha$ and amplitude $a_\rho = 0.2\ \rho_0$ on the density in the box, along the z direction: $\rho(z, t = 0) = \rho_0 + a_\rho \sin(k_{ini} z)$. The simulations are followed until $t_{fin} = 500$ fm/c, with a recommended time step of either $\Delta t = 0.5$ or 1.0 fm/c. Nine BUU-type and five QMD-type codes participated in the present comparison [6]. 10 events were considered for the BUU models, whereas 200 events were run for the QMD codes.

The Coulomb interaction and the nuclear symmetry force are turned off. For the non-relativistic codes, a standard Skyrme parametrization (without momentum-dependence) for the single-particle potential is used, $U(\rho) = a(\rho/\rho_0) + b(\rho/\rho_0)^\sigma$, with the following parameters: $a = -105.716\,\mathrm{MeV}$, $b = 52.836\,\mathrm{MeV}$, $\sigma = 2.587$. The nucleon mass is taken to be $M = 93\,\mathrm{MeV}$. This parameterization leads to the following nuclear matter properties: compressibility $K_0 = 500\,\mathrm{MeV}$, saturation density $\rho_0 = 0.16\,\mathrm{fm}^{-3}$ and the binding energy at saturation density $E_0 = -16\,\mathrm{MeV}$. For the relativistic codes, we employ a non-linear $\sigma - \omega$ Relativistic Mean Field (RMF) parameterization, leading to the same properties. Different options were considered for the Dirac effective mass m^*. Figure 1 (left panel) shows the energy per nucleon (a) as a function of the baryon density ρ, in the case of the Skyrme interaction, the pBUU model (including only a scalar field) [11] and three RMF parametrizations. In the case of the relativistic approaches, the Dirac mass m^* (b) and the scalar density (c) are also shown. The right panel of the figure shows the corresponding gradients of the mean-field potential, namely the quantity $-F(z) = \partial\epsilon/\partial z$, with ϵ being the single-particle energy, calculated analytically for the initial standing wave impressed on the density profile. In the case of the Skyrme interaction, one can simply write $-F(z) = \frac{\mathrm{d}U}{\mathrm{d}\rho}\cdot\frac{\mathrm{d}\rho}{\mathrm{d}z}$. As one can see in the figure, though all parametrizations give the same trend for the EoS around saturation density, as required, quite interesting differences exist for the gradient of the mean-field potential. This simply stems from the fact that different effective interactions may lead to the same EoS. In the following we will consider, for the RMF codes, the parametrization corresponding to $m^*/M = 0.9$, which gives gradient values closer to the Skyrme interaction (see fig. 1, right panel).

3˙1. *Momentum space.* – In fig. 2 we show the distribution of the absolute value of the particle momentum, $f(p) = (2\pi)^3 n(p)/(4V_{ps})$, where $n(p)$ is the number of nucleons with momentum p and V_{ps} represents the phase-space volume: $V_{ps} = V_{box}\cdot(4\pi p^2)\Delta p$. $V_{box} = L_\alpha^3$ denotes the volume of the box and we adopt $\Delta p = 5\,\mathrm{MeV/c}$. At the initial time, for homogenous matter at saturation density this distribution would be a step

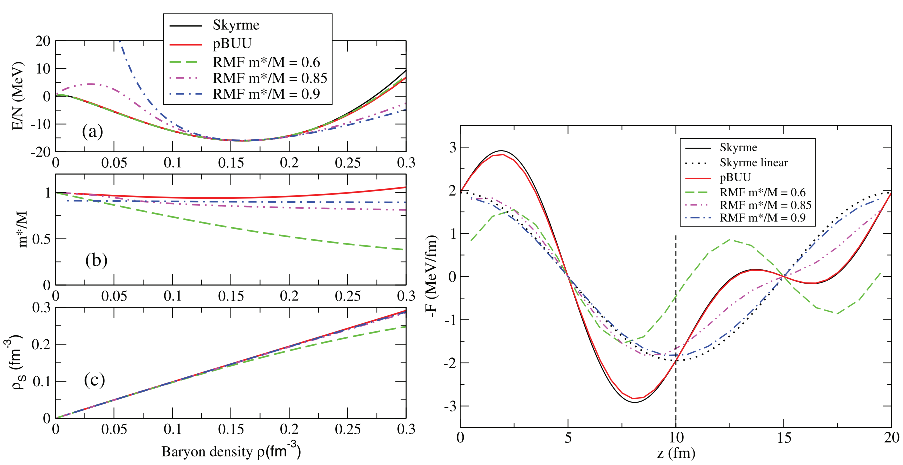

Fig. 1. – (Color online). Left panel: (a) Energy per nucleon, as obtained for the adopted Skyrme-like parametrization (full (black) line), three RMF parametrizations and for the pBUU model (thick full (red) line). Right panel: Corresponding gradient of the mean-field potential.

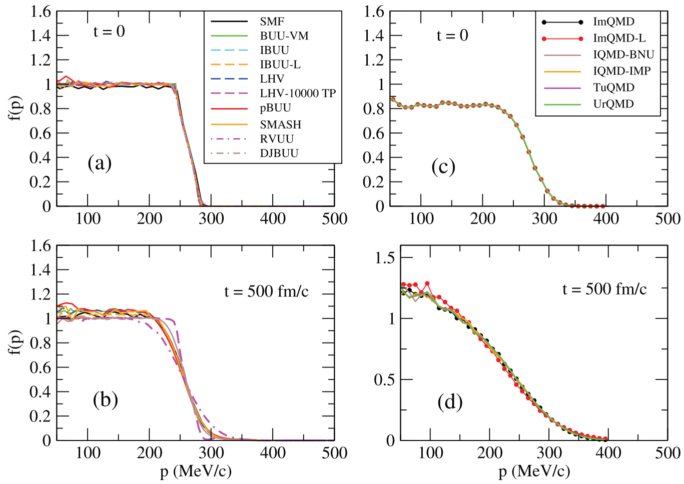

Fig. 2. – (Color on line). Momentum distributions in the different codes at initial ((a) and (c) panels) and final ((b) and (d) panels) times: BUU-like in panels (a) and (b) and QMD-like in panels (c) and (d).

function at the Fermi momentum of about 265 MeV/c. As observed for the BUU-like codes, there is a slight smearing, due to the impressed standing wave. For the QMD-like codes, a considerably larger smearing is seen, corresponding to the larger intrinsic initial density fluctuations (generating a wider range of local Fermi momenta). It should be noticed that all QMD codes have employed exactly the same input for initialization.

The results obtained by adopting the extreme choice of $N_{TP} = 10000$ in the (BUU-like) LHV calculations show that the initial momentum distribution should be approximately preserved in time. Indeed, in this case the final configuration is very close to the initial one. However, it is seen that in general the momentum distribution changes by amounts that depend on the code. Most BUU codes reasonably well preserve the quantum-statistical behaviour. The QMD-like codes in panel (d) are seen to deviate significantly from the Fermi statistics at the final time, approaching the classical Maxwell-Boltzmann distribution. This behavior can be ascribed to the larger fluctuations inherent to the QMD approach, that will also influence the density oscillations.

3˙2. *Strength and response functions.* – To characterize the density perturbation introduced in the initial conditions and its time evolution, it is useful to perform a Fourier analysis of the spatial density. We define the Fourier transform of the averaged density as $\rho_k(t) = \int_0^{L_z} \mathrm{d}z\, \rho(z,t)\, \sin(kz)$, which gives a more compact representation of the density profile and can be called the strength function of the k mode. One generally observes damped oscillations as a function of time for the latter quantity. We consider $k = k_{ini} = 2\pi/L_\alpha$. However, as time evolves, other k components can appear. This can be called mode-mixing, which is due to the non-linear character of the Vlasov equation, but also to fluctuations.

A deeper insight into the frequency and the damping of the density oscillations is obtained from a further Fourier analysis of $\rho_k(t)$ with respect to time, *i.e.*, the response function. Hence we introduce quantity $\rho_k(\omega) = \int_{t_{in}}^{t_{fin}} \mathrm{d}t \rho_k(t) \cos(\omega(t - t_{in}))$, where the integration is extended over a time interval $\Delta t_{fi} = t_{fin} - t_{in}$, with a suitable choice of

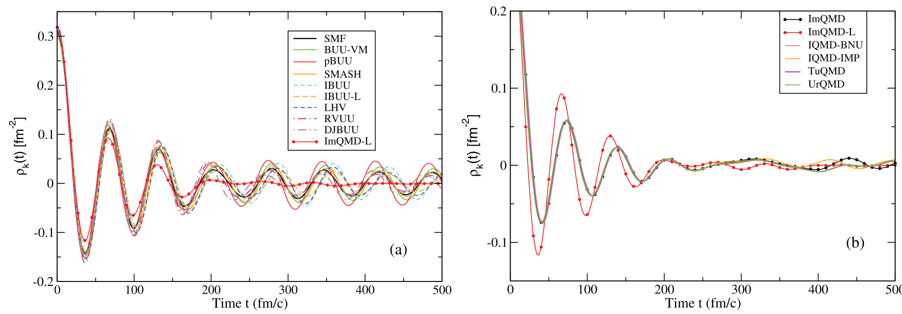

Fig. 3. – (Color online). Left panels: the strength function $\rho_k(t)$ for mode k_{ini} is displayed as a function of time. Results are shown for BUU-like calculations (left panel), including ImQMD-L calculations for comparison, and QMD-like calculations (right panel).

the initial time t_{in}. The peak of the response function indicates the oscillation frequency, whereas its width is connected to the damping of the density oscillations.

Figure 3 shows the results obtained for the time evolution of the strength function, for all codes involved in the comparison. One can observe that BUU-like codes give quite similar results. The differences observed are compatible with the different scheme (either fully covariant, non-relativistic or with only relativistic kinematics) of the different models. The QMD-like codes exhibit an excellent agreement among them, but a lower oscillation frequency and larger damping effects are observed with respect to the results of BUU-like codes. The lowering of the oscillation frequency stems from the approximate treatment of the many-body term of the nuclear interaction in QMD [12]. A more accurate treatment is found in recent formulations (see the results of the ImQMD-L code in the figure) adopting the Lattice Hamiltonian method to implement the mean-field dynamics [12]. Finally, fig. 4 summarizes the results, showing the response function obtained for all BUU-like codes and two representative QMD codes. Calculations were done considering, as initial time t_{ini}, the first minimum observed in the time evolution of the strength function.

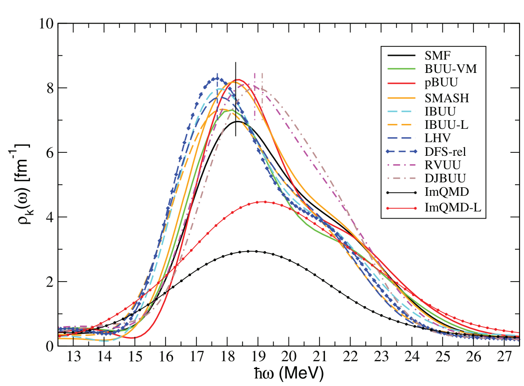

Fig. 4. – (Color online). Response function $\rho_k(\omega)$, *i.e.*, Fourier transform with respect to space and time, of the averaged density distribution from BUU-like and two QMD-like calculations. The vertical lines indicate the analytical zero-sound energies for the different code types, down-shifted by 2%.

4. – Conclusions

We report on a study of mean-field dynamics in a box, without collisions, comparing the results of several transport codes. The system is initialized in terms of a standing density wave and the system evolution is followed with different participating codes using energy functionals that are made identical or similar. Major transport codes from the two basic families, BUU and QMD, are included in this study, which also partly account for relativistic effects in different approximations. The comparisons include those of the strength function characterizing mode evolution and response function revealing how frequencies are tied to the modes. We find that we can generally understand consistencies and differences between the results of the codes. The differences among the codes and relative to near-exact results that persist include: 1) relativistic effects that yield observable effects in the frequency of collisionless mode; 2) approximations to the calculation of the non-linear terms of the force used in QMD codes that lead to noticeable differences in the frequency of the density oscillations even at early times, which can, however, be avoided in a lattice evaluation scheme; and 3) the importance of damping effects generated by statistical or numerical fluctuations. Indeed, the most noticeable differences in the results of the codes arise from the fluctuations inherent in the coarse phase space representation, which are characteristically different in BUU and QMD codes. These findings do not make a statement about the validity of the two approaches, since the physical modeling is different: QMD codes attempt to put a reasonable amount of fluctuation already into the ansatz for the representation, while in BUU these would have to be included by an extra fluctuation term in the Langevin framework. The findings for the long-term behavior are relevant to the uses of semiclassical transport in the studies of oscillations of isolated finite nuclei, including comparisons to quantum-mechanical calculations in TDHF and RPA [13].

REFERENCES

[1] Colonna M., *Prog. Part. Nucl. Phys.*, **113** (2020) 103775.
[2] Kolomeitsev E. E. *et al.*, *J. Phys. G*, **31** (2005) S741.
[3] Xu J. *et al.*, *Phys. Rev. C*, **93** (2016) 044609.
[4] Zhang Y. *et al.*, *Phys. Rev. C*, **97** (2018) 034625.
[5] Ono A. *et al.*, *Phys. Rev. C*, **100** (2019) 044617.
[6] Colonna M. *et al.*, *Phys. Rev. C*, **104** (2021) 024603.
[7] Xu J., *Prog. Part. Nucl. Phys.*, **106** (2019) 312.
[8] Ono A., *Prog. Part. Nucl. Phys.*, **105** (2019) 139.
[9] Aichelin J., *Phys. Rep.*, **202** (1991) 233; *Phys. Rev.*, **33** (1986) 537.
[10] Ayik S. and Gregoire C., *Phys. Lett. B*, **212** (1988) 269; *Nucl. Phys. A*, **513** (1990) 187.
[11] Danielewicz P., *Nucl. Phys. A*, **673** (2000) 375; Danielewicz P. and Bertsch G. F., *Nucl. Phys. A*, **533** (1991) 712.
[12] Yang J., Zhang Y., Wang N. and Li Z., *Phys. Rev. C*, **104** (2021) 024605.
[13] Burrello S. *et al.*, *Phys. Rev. C*, **99** (2019) 054314.